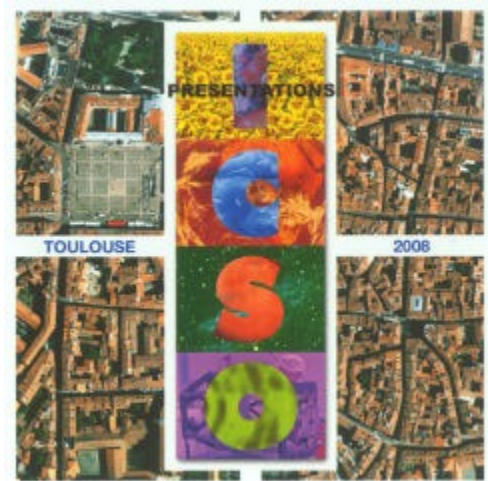


International Conference on Space Optics—ICSO 2008

Toulouse, France

14–17 October 2008

Edited by Josiane Costeraste, Errico Armandillo, and Nikos Karafolas



Development of an EMCCD for LIDAR applications

B. De Monte

R. T. Bell



International Conference on Space Optics — ICSO 2008, edited by Josiane Costeraste, Errico Armandillo, Nikos Karafolas, Proc. of SPIE Vol. 10566, 105662Q · © 2008 ESA and CNES
CCC code: 0277-786X/17/\$18 · doi: 10.1117/12.2308270

DEVELOPMENT OF AN EMCCD FOR LIDAR APPLICATIONS

B De Monte⁽¹⁾, R T Bell⁽²⁾,

⁽¹⁾e2v Grenoble, Avenue de Rochepleine, BP 123, 38521, Saint-Egrève Cedex, France, bertrand.DEMONTE@e2v.com

⁽²⁾e2v technologies, 106 Waterhouse Lane, Chelmsford, Essex, CM1 2QU, UK. ray.bell@e2v.com

ABSTRACT

A novel detector, incorporating e2v's EMCCD (L3Vision™) [1] technology for use in LIDAR (Light Detection And Ranging) applications has been designed, manufactured and characterised. The most critical performance aspect was the requirement to collect charge from a 120µm square detection area for a 667ns temporal sampling window, with low crosstalk between successive samples, followed by signal readout with sub-electron effective noise. Additional requirements included low dark signal, high quantum efficiency at the 355nm laser wavelength and the ability to handle bright laser echoes, without corruption of the much fainter useful signals.

The detector architecture used high speed charge binning to combine signal from each sampling window into a single charge packet. This was then passed through a multiplication register (EMCCD) operating with a typical gain of 100X to a conventional charge detection circuit. The detector achieved a typical quantum efficiency of 80% and a total noise in darkness of < 0.5 electrons rms. Development of the detector was supported by ESA.

1 INTRODUCTION

The CCD was designed for possible use as the detector in a space based LIDAR instrument with a 667ns temporal sampling window to give 100m spatial resolution. A simplified overview of the instrument and its operation is shown in Fig. 1. Use with a 355nm laser required a high quantum efficiency at ultra-violet wavelengths necessitating a back-illuminated CCD structure. Optical spot size and alignment issues required a 120µm square image area and a number of novel device concepts to extract charge from this detector area with low crosstalk between successive atmospheric samples were considered in the design phase. It was concluded that conventional charge binning in a two-stage process was the lowest risk approach.

2 CRITICAL DEVICE PARAMETERS

2.1 Quantum Efficiency

The system requires a high Quantum efficiency of >70% at 355nm. This was met by a back-illuminated CCD with e2v's standard (UV optimised) ion implantation and laser anneal back surface treatment, together with a customised anti-reflection coating. As the device is designed to detect UV wavelengths and has no demanding spatial resolution requirements the silicon thickness and resistivity are not critical for optical performance, and were chosen for optimum performance from the EM gain register.

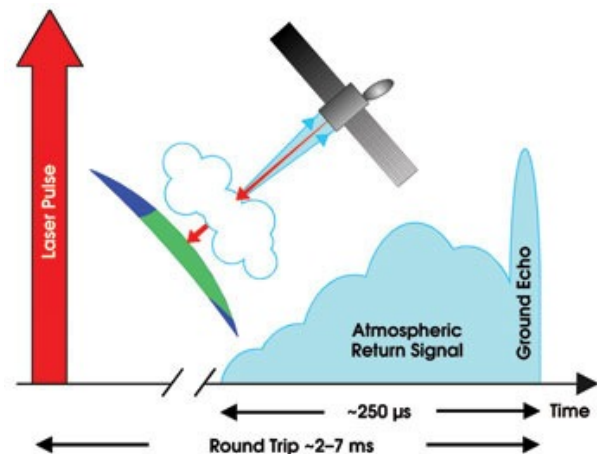


Fig. 1. LIDAR System Overview

2.2 Dark Signal

The required dark signal is less than 0.3 electrons per atmosphere sample in LIDAR mode. This low value influenced the choice of device architecture and led to concepts in which multiplication gain was applied to the signals as early as possible. This required the multiplication register to operate at a frequency of 1.5MHz to match the signal sampling rate. Architectures which stored the signals before multiplication at a lower clock rate were rejected. Even with the optimum architectures the predicted dark signal at +20°C was approximately 4 electrons per sample and this value was dominated by the contribution from the multiplication register.

Techniques such as 'Inverted Mode Operation' or dither clocking are not applicable to multiplication registers as the magnitude of the clock-induced charge generated in the multiplication register is increased dramatically under these conditions. Only two strategies are therefore available to meet the requirement. Firstly the CCD needs to be cooled to a temperature in the range -10°C to -20°C (the required value was confirmed by experiment in the programme). Secondly the width of the multiplication register, and hence the dark current generation area, was reduced at the input end where signal levels are small and tapered out to a normal value towards the output end, to accommodate the increasing signal.

2.3 EM Gain Register (Multiplication Register)

In order to achieve the required noise performance it was predicted that multiplication gains in the range from 50 to 200 would be required. This range is readily achieved with a similar gain register to that used on previous e2v technologies designs using typically 500 multiplication stages. Apart from the tapering of register width discussed previously the register is therefore of conventional design, similar to that used on the CCD97 for example.

The stability of the multiplication gain was reviewed as this depends on temperature and on the operating voltages, being a very strong function of the amplitude of the high voltage clock pulse ($R\theta 2HV$). Analysis of results from other devices suggested that a temperature stability of $\pm 0.25^{\circ}\text{C}$ and a voltage stability of 4mV would be necessary to achieve the required gain stability. Part of the characterisation phase of the programme was to demonstrate that these levels were achievable.

Comparison with other devices also suggested that the required levels of linearity should be achievable with a standard register design for the system signal levels and the range of gains discussed above.

To allow calibration of the multiplication gain and measurement of linearity an electrical input structure at the start of the gain register was proposed, based on similar structures which had been used on test devices produced by e2v. Electrical input was preferred rather than optical methods as it allows better control and charge measurement for calibration.

It is known that for a fixed high voltage register clock amplitude, the on chip multiplication gain drops as the device is run [2]. This process is known as ageing and depends on the total quantity of charge transferred through the multiplication register. In order to maximise the useful life of the sensor it is important to ensure that

only the wanted signals are passed through the register. The low duty cycle of the system, 400 signal samples in 10ms, should then ensure a tolerable level of ageing over the mission lifetime.

2.4 Antiblooming and Dump Drains

Various drain structures are required in the device to remove unwanted or excess signals. Antiblooming drains cannot be included in the image section as a requirement to measure the brightness of the locally reflected 'signal at laser emission' was included in the specification. This signal is likely to exceed the capacity of the image section pixels but may still be measured if the bloomed signal in several pixels is added together. An antiblooming drain along the gain register (similar to other EMCCDs) can be used to limit excess signals in the multiplication register, e.g. from specular echoes, and prevent such signals corrupting useful data or ageing the register excessively.

Dump drain structures, similar to those used on standard imaging CCDs, can be used to remove the 'signal at laser emission' if it is not to be measured.

2.5 Collection of Signal from 120 μm Detector

Charge generated within the 120 μm square detector area in a 667ns interval must be combined into a single CCD element at the input of the gain register. This process must minimise the crosstalk between successive temporal samples. Charge transfer across a single pixel of this dimension would be extremely slow, particularly at the very low signal levels ($\sim 1e^{-}$ per sample) down to which the sensor was required to operate. A number of architectures to achieve the required performance were considered but it was concluded that the lowest risk was the use of conventional clocked binning of charge in an array of smaller pixels. This has the secondary advantage that the sensor area can be operated in a conventional imaging mode for alignment purposes etc. The number and size of the pixels into which the detector is divided was determined by the trade off between clock frequency and transfer efficiency. A larger number of smaller pixels requires a higher clock frequency to read out in the available time. A smaller number of larger pixels will have decreased transfer efficiency due to the slower charge transit time, which increases approximately as the cube of the pixel dimension. A 6 x 6 pixel array of 20 μm square pixels was calculated to be optimum. This pixel size allows clocking at 24MHz with good transfer efficiency, which enables six image and two overscan pixels to be binned within a 667 ns sample period, with sufficient time remaining for the other clocking which is required.

For typical levels of charge transfer efficiency the crosstalk between successive temporal samples of the optical signal is dominated by the 'frame shift smear' in the image section. A model was developed to calculate this for a range of optical spot sizes and positions and confirmed that the specified value of 13% could be met.

3 DEVICE ARCHITECTURE

The architecture of the device is shown in Fig. 2 and described in the following sections.

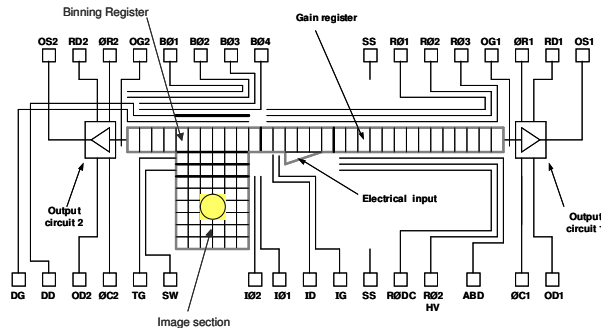


Fig. 2. Detector Architecture

3.1 Image Section

The image section consists of a central 6 x 6 pixel array with additional rows and columns to minimise edge effects. Charge from the additional columns on each side is directly dumped to drains next to the binning register (not shown in the schematic). The image section has a total of 10 rows with the photosensitive region defined by a metal light shield, which is deposited directly on the CCD. Two-phase clock electrodes are used to simplify the high speed clocking required to perform charge binning. Charge from the whole image section is binned into a summing well (SW) adjacent to the binning register but isolated from it by a separately clocked transfer gate (TG).

3.2 Binning Register

The binning register receives signal charge from the image section and is clocked to bin a row of charge into the first element of the gain register. The binning register has a four-phase electrode structure incorporating the barrier implants used for two-phase electrodes. This allows bi-directional charge transfer with simple two-phase clock waveforms by appropriately pairing electrodes. Charge transfer in the reverse direction (without binning) is used when the device is operated in a simple imaging mode. A gated dump drain along the side of the binning register allows any unwanted signals to be dumped directly without transfer through the multiplication register.

3.3 Multiplication Register

The multiplication register is typical of that used in other e2v EMCCDs except for the reduced width at the input end, as discussed above. It consists of 520 multiplication stages with additional non-multiplying stages at both ends, as is standard. An antiblooming drain runs the full length of the register to remove excess charge from any very bright signals.

3.4 Output Circuits

The device includes two independent output circuits of nominally identical performance. Output 1, the gain register output, is used in LIDAR mode while output 2 at the other end of the binning register is used in imaging mode e.g. for alignment or for measurement of the bright locally reflected 'signal at laser emission'. The two outputs have a nominal responsivity of 3 μ V per electron, are capable of operation at 1.5MHz clock rate and have a read noise of 10 electrons rms. at this rate.

3.5 Charge Injection Structure

The charge injection structure consists of an input diode and a separate control gate. It is typically used in conjunction with a precision current source to inject a known quantity of charge into the gain register on each clock cycle. The multiplication gain is then measured directly as the ratio between the signal current at the output of the gain register (reset drain current) and the input current. The charge injection circuit may be turned off completely when not required by applying a suitable positive bias (+20V typical) to the input diode.

4 LIDAR MODE OPERATING SEQUENCE

An overview of the LIDAR mode operation is shown in Fig. 3 while Fig. 4 shows details of the clock sequence used in the acquisition period when signals are binned from the image section into the multiplication register. During the 'stand-by' period the image section is clocked with the dump gate held high to clear unwanted charge to the dump drain. In the 'acquisition' period photogenerated charge is integrated in the image section and then rapidly binned vertically into the summing well. This integration and binning occur in a first 667ns sample period. During a second sample period, while the second sample signal is integrated, the first sample is transferred to the binning register. The first sample is then binned horizontally into the gain register while the second sample is binned into the summing well. During each following sample period the first sample signal is advanced one stage along the gain register and multiplied. When the required set of 400 samples have been acquired into the multiplication register the device is switched to 'readout' mode. In this mode the clocking

of the multiplication register continues with the same timing but the image and binning register clocks are stopped to avoid feedthrough into the output video waveform.

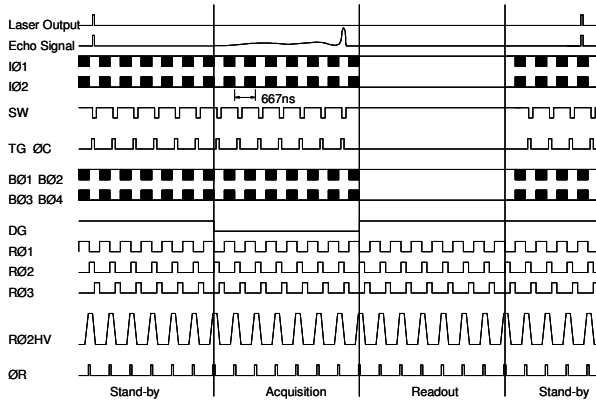


Fig. 3. LIDAR Mode Overview

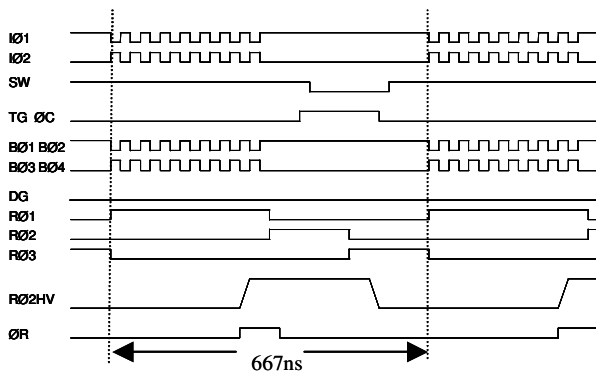


Fig. 4. LIDAR Acquisition mode Clock Sequence

After readout is completed the device returns to 'standby' mode. The multiplication register is clocked continuously with a constant duty cycle throughout the entire sequence in order to facilitate maintaining a stable amplitude of typically 40V, as required to give a gain of 100X.

5 PACKAGE DESIGN

The package used for this development phase was not required to be a flight package. The principal requirement was to allow a simple means to maintain a stable device temperature of -10°C to -20°C for testing. The package was therefore based on a standard part used by e2v for other EMCCDs. It is a kovar-bodied package with an internal single-stage Peltier cooler.

A photograph of the CCD in its package is shown in Fig. 5.

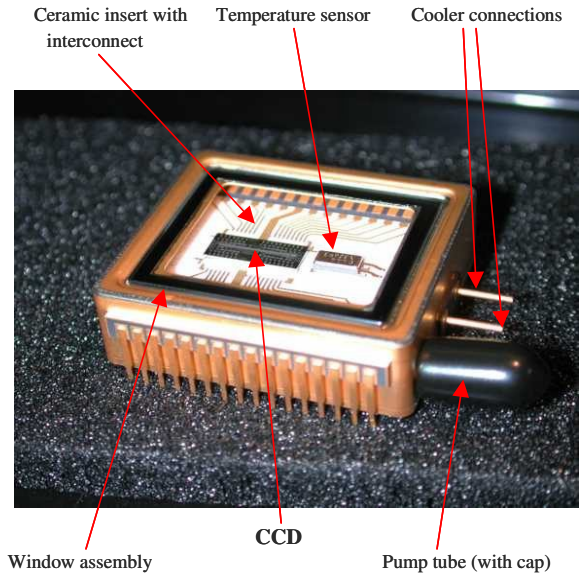


Fig. 5. LIDAR CCD in package

The CCD die and a temperature sensor sit on a ceramic insert, mounted on the cold face of the cooler, with metallised tracks to connect to the package pins. The package has a sapphire window which is antireflection coated to give less than 1% reflection at 355nm. The package has an integral pump tube and is fully processed before sealing.

6 DEVICE MANUFACTURE

Wafer batches of sensors were processed in the e2v technologies wafer fabrication area in Chelmsford, using the standard 4-level polysilicon manufacturing process used for other EMCCDs. Basic device functionality was demonstrated on front illuminated samples initially then further wafers received the additional processing required for back-illuminated devices. This included deposition and patterning of a light shield to cover all but the 6×6 pixel image area with a 1 pixel border.

7 DEVICE PERFORMANCE

The electro-optic performance of a number of back-illuminated devices was assessed at e2v technologies using an engineering test camera with a specially built light source, which produced a simulated LIDAR echo signal. The source used two LEDs and a laser diode which could be independently pulsed with a range of currents under control of the CCD clock sequencer to give a wide range of signal levels and patterns.

7.1 Multiplication Gain

The high voltage clock pulse amplitudes required to give gains of 50 and 200X at -20°C and a gain of 100X

at -20°C , -15°C and -10°C were measured. These operating conditions were used in subsequent tests to determine the recommended operating point, which was part of the objective of the characterisation. All devices were very similar requiring typically 40V for 100X gain at -20°C , which was the final recommended condition.

The stability of the multiplication gain was measured as the peak to peak range of the mean signal level of each set of 400 signal samples (equivalent to the echo from a single laser pulse) over a 15 second period in LIDAR mode with constant illumination from one of the LED light sources. The measured value of $\pm 0.8\%$ exceeds the specification of 1%. However a review of the measurement established that the variation in mean level of the 400 samples was dominated by the random noise component due to photon shot noise and the excess noise factor (see section 7.4). Calculation of the average signal over successive sets of 4×400 samples gave a gain stability within specification. This demonstrated that the required levels of voltage and temperature stability are achievable.

7.2 Quantum Efficiency

The quantum efficiencies (QE) of two typical devices at 355nm were 81.8% and 81.6% which met the specification of $>70\%$ with some margin. However it was observed that another device sample showed some instability of quantum efficiency over time and an investigation was carried out. It was concluded that the most likely explanation of the changes seen is that volatile contamination is condensing on the CCD when it is cooled.

7.3 Total Noise in Darkness

The total noise in darkness, which includes the contribution of dark current shot noise, was measured for the same set of operating conditions as the multiplication gain. Typical values were 0.43e- rms per sample. for 100X gain at -20°C with significantly higher values for lower gain or higher temperature and only a slight decrease at 200X gain and -20°C .

The contribution of readout noise to the total was approximately 0.15e- rms as the effective contribution from the amplifier and system (15e-) is reduced by the gain of the multiplication register.

7.4 Excess Noise Factor

When multiplication gain is employed, there is an additional contribution to the noise due to the stochastic nature of the charge multiplication process. The excess noise factor, F , is defined as the input referred noise with gain divided by the input referred noise without

gain, under conditions of zero readout noise. If in the multiplication process each signal electron is assumed to behave independently of all the other signal electrons, it can be shown that, for large multiplication gain [3].

$$F = \sqrt{2/(1 + \alpha)} \quad (1)$$

where α is the probability of multiplication gain per stage. Since the CCDs have 520 multiplication gain stages, $\alpha \ll 1$, and this gives $F = \sqrt{2}$.

The excess noise factor from the multiplication process was measured for a range of signal levels with a gain of 100 and was close to the theoretically expected value of $\sqrt{2}$ for small signals. However for input signal levels above approximately 400e- the value decreased. To investigate this effect, measurements of the excess noise factor were made for different multiplication gains and it was observed that the input signal level up to which the full excess noise was seen decreased with increasing gain. The break point corresponded approximately to a constant output signal level. It was therefore suspected that the effect was due to signal charge coming into contact with traps at the silicon surface. Such trapping and subsequent release of charge would be expected to have a smoothing effect on the excess noise. Trapping would also give rise to charge transfer inefficiency (CTI) and so measurements of this were made for a range of gains and signal levels. Typical results are given in Fig. 6 which shows the residual signal in successive dark samples following a block of 400 illuminated samples in LIDAR mode at a range of signal levels. It is clear that the trap release time constant becomes longer at larger signal levels. Charge interaction with these slow traps would have a more significant smoothing effect on the excess noise.

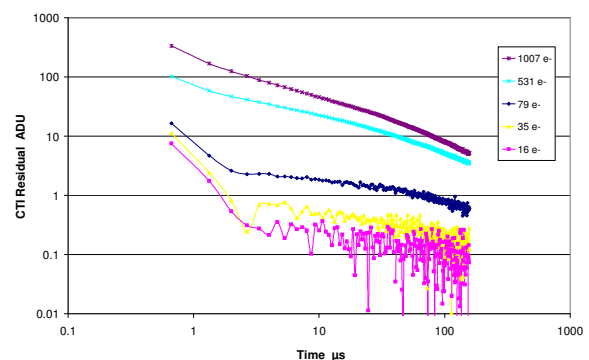


Fig. 6. CTI decay profile vs. input signal level.

In parallel with this device development, other work at e2v showed that the design of the multiplication register elements was not optimised and small changes to the

layout can give significant increases in the signal level which can be transferred and multiplied without contact with surface traps.

7.5 Dark Signal

The dark signal in LIDAR mode cannot be measured directly but was estimated from the Total Noise in Darkness, the readout noise and the excess noise factor. The estimated dark signal was less than 0.1 electrons per sample at -20°C with 100X gain, which meets the specification of <0.3 electrons.

7.6 Crosstalk

The crosstalk performance of $< 1.7\%$ which was measured at a signal level of $500e^-$ per sample is well within specification of $<13\%$. This value is achieved with a $20\mu\text{m}$ diameter light spot positioned centrally in the image section and with a 667ns optical pulse starting and finishing at approximately the middle of a 'frame transfer' As the spot is moved vertically either the leading or trailing crosstalk increases, in line with the predictions of the model.

7.7 Linearity

Under the recommended operating condition a linearity error of $<1\%$ was maintained for input signal levels up to $1300e^-$ at $\times 100$ gain which covers the specified range of atmosphere sample signals. The 'normal ground echo' signal defined as $1900e^-$ was handled with a linearity error of no more than 4% .

Some additional linearity measurements were also performed to investigate linearity down to very low signal levels. The use of the charge injection circuit is restricted to moderate signal levels by the presence of leakage currents.

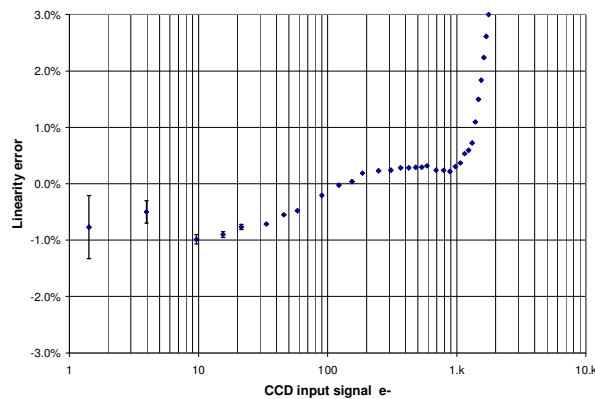


Fig. 7. Linearity error vs. input signal level at $\times 100$ gain

An alternative measurement based on optical inputs was therefore devised. The results of this measurement are shown in Fig. 7, which confirms that good linearity performance is maintained down to very small input signals.

7.8 LIDAR Mode Demonstration

The performance of the CCD in LIDAR mode was demonstrated using various signals generated by the pulsed optical source to simulate atmospheric, local and ground echoes. An example is shown in Fig. 8.

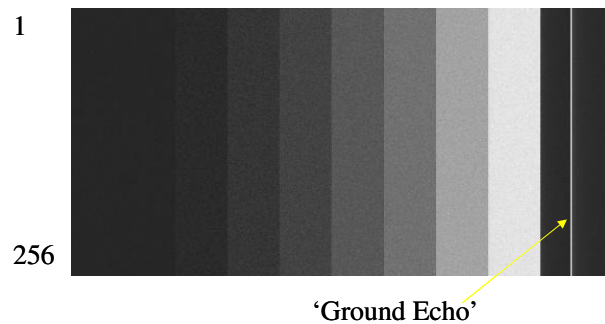


Fig. 8. LIDAR Mode Demonstration with Normal Ground Echo

This shows 256 successive acquisitions during each of which the signal level from the LEDs was increased in a series of steps, acquiring 50 samples at each signal level, followed by a short pulse (20ns duration) from the laser diode to simulate the ground echo.

7.9 Ageing

All previous characterisation of ageing had been performed on TV type sensors at room temperature. A basic characterisation of ageing under representative LIDAR system conditions was therefore carried out on these devices.

The ageing tests were performed on four front illuminated devices. These were characterised before and after the ageing using a sub-set of the tests performed on the back illuminated devices.

During the ageing period one pair of devices, designated A and B, were operated with constant $R_{\text{O}2\text{HV}}$ amplitude and their multiplication gain was monitored. The second pair of devices designated C and D were operated at nominally constant gain of 100X with $R_{\text{O}2\text{HV}}$ being adjusted at each measurement point to restore the gain.

The devices were operated at -20°C and illuminated with a pulse of light to give a signal equivalent to the ground echo every 10ms. After an ageing period of

2700 hours the pulse rate was increased by a factor of 10 for a further 914 hours in an attempt to accelerate the ageing. Plots of gain or required high voltage clock amplitude against equivalent time (scaled by a factor of 10 in the second period) showed a continuous gradient across the transition indicating that the acceleration of ageing was as expected. Sample results for devices A and B are shown in Fig. 9.

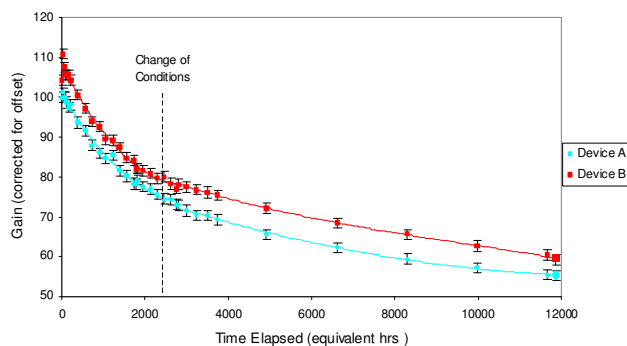


Fig. 9. Ageing of devices at constant clock amplitude.

The change in gain could be recovered by an increase in clock amplitude of approximately 1V. After adjustment of the clock voltage the electro-optic properties of the devices were substantially unchanged. Experience with other devices suggests that a maximum change of 5V is acceptable before device performance degradation occurs and this leads to a predicted lifetime of approximately 9 years in a LIDAR system.

8 CONCLUSIONS

This development has demonstrated the potential for L3Vision™ technology to deliver sub-electron levels of total noise in darkness together with adequate gain stability to allow its use in measuring instruments to be considered. Other electro-optic properties typical of standard CCDs can be maintained.

9 REFERENCES

1. P.Jerram et al. The LLLCCD: Low light imaging without the need for an intensifier. Proc. SPIE vol.306 pp. 178-186, 2001.
2. e2v technologies Low Light Technical Note 5 An Overview of the Ageing Characteristics of L3Vision™ Sensors <http://www.e2v.com>
3. M S Robbins, B Hadwen, The Noise Performance of Electron Multiplying Charge-Coupled Devices. IEEE Transactions on Electron Devices Vol. 50 no. 5 May 2003